Comparative Dielectric Studies of Segmental and Normal Mode Dynamics of Poly(oxybutylene) and Poly(oxyethylene)−Poly(oxybutylene) Diblock Copolymers

Apostolos Kyritsis,[†] Polycarpos Pissis,*[,†] Shao-Min Mai,[‡] and Colin Booth[‡]

Physics Department, National Technical University of Athens, Zografou Campus, 15780 Athens, Greece, and Manchester Polymers Center and Department of Chemistry, University of Manchester, Manchester M13 9PL, U.K.

Received March 23, 1999; Revised Manuscript Received February 18, 2000

ABSTRACT: Diblock copolymers of ethylene oxide and 1,2-butylene oxide, $E_{30}B_n$, with constant E-block length of 30 units and various B-block lengths ($n = 3-30$) were investigated, in parallel with a series of homopoly(oxybutylene)s of similar to B-block lengths, using broad-band dielectric relaxation spectroscopy ($10^{-2}-10^{9}$ Hz). The normal mode relaxation process due to reorientation of the end-to-end vector and the main (segmental) process caused by local chain motions, exhibited by the B-blocks in the copolymers and by the homopoly(oxybutylene), were studied in comparison to each other. The dynamics of the free chains in the liquid homopolymers is described more appropriately by the Rouse model, whereas the B-blocks in the crystallized copolymers exhibit significantly different dynamics. The results show that the B-blocks in the copolymers, constrained between lamellar crystals created by E-blocks, are more oriented and expanded, as compared to the chain conformation of the homopolymers. Comparative study of normal mode and main relaxations reveals, only for the homopolymers, a correlation length ξ for the main process on the order of 1−2 nm at temperatures close to the glass transition temperature, T_g.

1. Introduction

Dielectric spectroscopy is a powerful tool for studying molecular dynamics and conformational properties of polymers.[1,2] Among the various dielectric relaxation processes, exhibited by most dipolar amorphous polymers, the well-known α (or main) relaxation has been widely studied.[3,4] The main relaxation arises from the segmental motion and reflects the micro-Brownian motion of the polymer chain. If a chain unit has a dipole moment aligned parallel to the chain contour, this gives rise to the so-called dielectric normal mode process.[5−10] The normal mode process (n relaxation) is related to the fluctuation and orientation of the end-to-end polarization vector of the chain.

The most extensively studied polymer with respect to its normal mode process is *cis*-polyisoprene in the bulk amorphous state[7,8,11] and in solution.[12,13] High cis-content polyisoprene has proved to be an excellent dielectric probe, possessing dipolar moments both parallel and perpendicular to chain contour. Using dielectric spectroscopy, the dielectric response involving fluctuations of the end-to-end vector of *cis*-polyisoprene can be easily distinguished from the high-frequency segmental modes of the same chain as well as from relaxations of polymer chains of different molar mass. Because of this property of *cis*-polyisoprene, several dielectric investigations involving this polymer have been carried out, including studies on polyisoprene/polyisoprene blends,[14,15] polyisoprene/polybutadiene blends,[14,16] diblock and triblock copolymers with polyisoprene as a component,[17−19] and star polymers with polyisoprene arms.[20−22] Using dielectric spectroscopy, it was possible to extract the polyisoprene chain dynamics and to test several proposed molecular theories of polymer chain dynamics in blends and block copolymers.

This paper is concerned with polyethers. The first dielectric investigation of normal mode and main processes in this area was of the bulk amorphous state of poly(propylene oxide) (PPO) and was carried out in the 1960s by Bauer and Stockmayer.[5,6] Since that time PPO has been widely studied by dielectric spectroscopy (refs 9, 23−25 and references therein). Our present interest is in poly(1,2-butylene oxide) and in its block copolymers with poly(ethylene oxide). A limited range of these materials are available from the Dow Chemical Co., Freeport, TX,[26,27] but the diblock copolymers studied in this work were prepared in our laboratory. The two components are denoted E and B, where E represents an oxyethylene unit [OCH_2CH_2] and B an oxybutylene unit [$OCH_2CH(CH_2CH_3)$]. They have one crystallizable E-block and one atactic (amorphous) B-block.[28−31]

The useful properties of block copolymers originate largely from the tendency of blocks to segregate, giving rise to microdomain structures.[18,28,29] Consequently, there is much interest in investigating their structures in the bulk state, and a variety of experimental methods have been used. In this respect, extensive studies of the structures of EB-diblock copolymers have been made by simultaneous small-angle and wide-angle X-ray scattering (SAXS/WAXS) coupled with differential scanning calorimetry (DSC), by Raman spectroscopy, by rheology, and by atomic force microscopy (AFM).[30−34] Related studies have been made of EB-diblock copolymers in dilute aqueous solution, where they associate to form micelles, and in more concentrated solution where the micelles pack to form liquid-crystal gels.[35] However, present interest lies with the bulk state, and in particular with the semicrystalline solid state, since the copolymers chosen for this study form only disordered melts above their melting points.[30,32]

The work concerns a series of copolymers with constant E-block length (30 ± 4 E units) and various B-block lengths (3−30 B units). Yang et al.[30] investigated the structure of these copolymers in the semicrystalline state by means of simultaneous SAXS/WAXS/DSC techniques and low-frequency Raman

[†] National Technical University of Athens.
[‡] University of Manchester.

10.1021/ma990429e CCC: $19.00
Published on Web 05/24/2000

spectroscopy. For short B blocks (B_n, $n \leq 13$ B units) they found that unfolded E-blocks crystallized into lamellar crystals, and the noncrystalline B-blocks were also constrained to an unfolded conformation. For the longest B-block (B_{30}), it was shown that the unfolded conformation became unstable, leading to the formation of lamellae containing once-folded E-blocks while the B-blocks remained unfolded. Copolymers with intermediate block lengths form mixed lamellae containing extended and folded E-blocks. These effects were attributed to the difference in cross-sectional area of the two chains (E_m, 21 Å^2; B_n, 34 Å^2), coupled with the need to fill space at approximately normal density.[30,32]

The main purpose here is to report new results on these copolymers obtained from investigations of their dynamics by means of dielectric relaxation spectroscopy. In the solid state we extract information about the structure and conformation of the subchains by investigating the molecular motions of the B-blocks. The E-blocks being in crystalline state do not exhibit long scale molecular mobility. This complements the investigations of the overall solid-state structure mentioned above. Poly(butylene oxide) has a dipolar moment along the chain axis and exhibits the normal mode process in addition to the main process. Thus, for EB copolymers, dielectric spectroscopy can be a powerful investigative tool. Study of the conformations of B-blocks of various lengths, and of their molecular mobility, can provide information on the constraints imposed on the amorphous B-blocks by the crystallization of the E-blocks into a lamellar structure, as well as on other aspects of the structure−property relationships. In addition, the series of $E_{30}B_n$ copolymers investigated in this work were well-suited to a fundamental investigation of the dynamics of the normal relaxation of B-blocks through comparison with the normal mode relaxation of a series of homopoly(oxybutylene)s of similar length.

We have applied dielectric relaxation spectroscopy across wide ranges of frequency (10^{-2}−10^9 Hz) and temperature (205−400 K). Thus, through our investigation, we use the B-chain as a dielectric probe forced by electric fields which cover a wide range of length and time scales. Consequently, we study molecular mobility which is controlled by very different length scales, so that we are able to study the normal mode as well as the main process. The B-chains have various lengths and are in two different environments, i.e., in the liquid state as free chains and in the solid state constrained in microdomains by crystallization of the E-blocks. Taking advantage of this, it is an additional objective of the present paper to investigate the relationship between these two processes, a question which has been addressed over many years.[5,6,11,18,23,36−39] Any information obtained could shed light on the vitrification process in condensed matter.

Background. It is well established that fundamental features of the normal mode relaxation are described by a local correlation function that represents orientational correlation of two segments at two separate times:[12,22]

$$C(n,t;m) = \frac{1}{a^2}(\mathbf{u}(n,t)\cdot\mathbf{u}(m,0)) \qquad (1)$$

with $\mathbf{u}(n,t)$ being a bond vector for the nth segment at time t and $\alpha^2 = \langle u^2 \rangle$. For a chain composed of N segments, $C(n,t;m)$ can be decomposed into its eigenmodes at long time scales of the global motion:[22]

$$C(n,t;m) = \frac{2}{N}\sum_{p=1}^{N} f_p(n)\, f_p(m)\, \exp(-t/\tau_p) \qquad (2)$$

where f_p and τ_p are the eigenfunction and relaxation time, respectively, for the pth eigenmode ($p = 1, ..., N$). Correspondingly, at low frequencies ($\omega = 2\pi f$), the dielectric loss due to the normal mode relaxation can be written as

$$\frac{\epsilon''(f)}{\Delta\epsilon} = \sum_{p=1}^{N} g_p(N)\frac{2\pi f\tau_p}{1 + (2\pi f)^2\tau_p^{\,2}} \qquad (3)$$

where the intensity of the pth dielectric mode is given by

$$g_p(N) = \frac{2}{N^2}\left(\int_0^N f_p(n)\, \mathrm{d}n\right)^2 \qquad (4)$$

Thus, $\epsilon''(f)$ reflects features of chain dynamics through $f_p(n)$ and τ_p.

For low molar mass (unentangled) polymers at high temperatures compared to their glass transition temperature, T_g, the normal modes of chains and their viscoelastic and dielectric properties are in good agreement with the modified Rouse model for bulk polymers.[40,41] The model predicts that $f_p(n) \propto \sin(p\pi n/N)$ and $\tau_p \propto p^{-2}$, so that the dielectric loss can be written as

$$\frac{\epsilon''}{\Delta\epsilon} = \frac{8}{\pi^2}\sum_{p:\mathrm{odd}} \frac{2\pi f\tau_p}{p^2(1 + (2\pi f)^2\tau_p^{\,2})} \qquad (5)$$

Note that in eq 5 only odd-numbered modes with a characteristic time $\tau_p = \tau_1/p^2$ and an intensity proportional to p^{-2} are important.[10,41] It is worth mentioning here that several models proposed for the description of the chain dynamics, in the nonentanglement and in the entanglement regime as well, assume similar sinusoidal eigenfunctions $f_p(n)$. Thus, all models predict the same distribution of the normal eigenmodes and, consequently, almost identical shapes for the $\epsilon''(f)$ spectra at low frequencies. However, the span of relaxation times τ_p (τ_p/τ_1) is different among the theoretical models. For very low and very high frequencies compared to the frequency of maximum loss, the Rouse model predicts for the form of the dielectric loss curve, $\epsilon''(f)$:[41]

$$\epsilon''(f) \propto 2\pi f\tau_1 \sum_{p:\mathrm{odd}} p^{-2}, \quad 2\pi f\tau_1 \ll 1$$

$$\epsilon''(f) \propto (2\pi f\tau_1)^{-1/2}, \quad 2\pi f\tau_1 \gg 1 \qquad (6)$$

The dielectric relaxation strength $\Delta\epsilon$ for the normal relaxation of a chain with mean square end-to-end length $\langle R^2 \rangle$ is given by[42,43]

$$\Delta\epsilon = \frac{4\pi\mu^2}{(4\pi\epsilon_0)3kT}\frac{N_A\rho}{M}\, g_k \quad \text{(SI units)} \qquad (7)$$

with $\mu^2 = \mu_u^2\langle R^2 \rangle$, where $\boldsymbol{\mu}_\mathbf{u}$ is the dipolar moment per unit contour length of the chain, ρ is the density of the bulk polymer, N_A is the Avogadro constant, M the molar mass (for a polydisperse polymer this should be the weight-average value[10]), kT the thermal energy, and g_k

Table 1. Molecular Characteristics of B Homopolymers and EB Copolymers

	M_w/M_n	M_n/g mol^{-1}	$M_{n,B-block}$/ g mol^{-1}	ϕ_B[a]	melting range/K
		Homopolymers			
B_6	1.04	460			
B_{14}	1.03	970			
B_{25}	1.03	1810			
B_{63}	1.13	4500			
		Copolymers			
$E_{32}B_3$	1.04	1620	220	0.163	304−320
$E_{30}B_7$	1.03	1820	500	0.306	295−314
$E_{32}B_{10}$	1.03	2130	720	0.371	303−317
$E_{26}B_{13}$	1.08	2080	940	0.489	291−311
$E_{27}B_{17}$	1.06	2410	1220	0.544	293−312
$E_{29}B_{20}$	1.08	2710	1440	0.566	293−314
$E_{31}B_{30}$	1.06	3520	2160	0.647	292−311

[a] ϕ_B is the volume fraction of poly(butylene oxide) in the copolymer melt ($\phi_B = 1 - \phi_E$).[28,30]

the dipole correlation factor introduced by Kirkwood.[42] For the normal mode process g_k is usually taken as 1.[11,13] Equation 7 is obtained for the chains that have an isotropic orientational distribution and relax completely at sufficiently long times.

Regarding the molar mass dependence of relaxation times, specifically for τ_1 (the longest relaxation time), the Rouse model predicts, for unentagled flexible-linear chains, a power law expression of the form

$$\tau_1 \propto M^s \tag{8}$$

with $s = 2$. In many studies the exponent s has been found to be larger than 2, especially for polymers with entangled chains.[8,11,10,15,18] Many theories have been proposed for entangled systems based mostly on the original tube model proposed by de Gennes[44] and by Doi and Endwards.[41] The tube model predicts a similar molar mass dependence of τ_1 (the so-called reptation time) but with exponent $s = 3$. As a general rule, experimental findings of a power law dependence of τ_1 on M with $s > 2$ are attributed to increased interactions among the chains, e.g., entanglement for high M or hydrogen bonding for chains with relatively low M.[9,10,15]

2. Experimental Section

2.1. Copolymers. The copolymers were prepared by sequential anionic polymerization, first of ethylene oxide and then of 1,2-butylene oxide, and starting from the monomethyl ether of ethylene glycol partly in the form of its potassium salt. The methods of preparation and characterization have been described in detail previously.[45] The molecular characteristics of the copolymers are listed in Table 1.

2.2. Homopolymers. Three samples of α-hydro-ω-hydroxypoly(oxybutylene) [polybutylene glycol, PBG) were obtained as a generous gift from Dr. V. M. Nace, The Dow Chemical Company, Texas Operations. Characterization by GPC and ^{13}C NMR gave values of M_w/M_n and M_n in good agreement with those supplied. A fourth sample was prepared in our laboratory using the general method described in section 2.1 but initiating the polymerization with 1,2-butanediol. The molecular characteristics of the polymers are listed in Table 1.

2.3. Dielectric Relaxation Spectroscopy. The dielectric measurements covered the frequency range from 10^{-2} to 10^9 Hz. For measurements in the frequency range 10^{-2}−10^6 Hz the sample was kept between two gold-plated brass electrodes (diameter 20−30 mm) with a spacing of 50 μm maintained by fused silica fibers. Two different measurement systems were used in this frequency range: (1) a Solatron-Schlumberger frequency response analyzer FRA 1260 with a buffer amplifier of variable gain and working frequency range 10^{-2}−10^6 Hz;

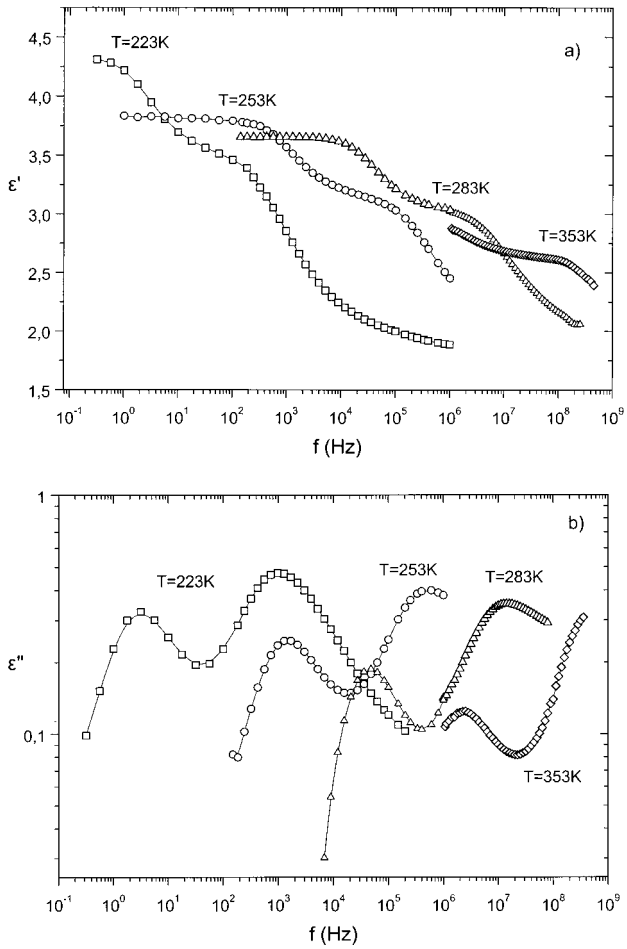

Figure 1. Semilogarithmic frequency plots of real part $\epsilon'(f)$ (a) and double-logarithmic frequency plots of imaginary part $\epsilon''(f)$ (b) of the dielectric permittivity $\epsilon^*(f)$ at several selected temperatures for homopolymer B_{63}.

(2) a Hewlett-Packard precision LCR meter, 4284A, with working frequency range 20−10^6 Hz. The temperature of the sample was controlled by an Ando type TO-19 thermostatic oven, in the range 210−330 K.

For measurements in the frequency range 10^6−10^9 Hz a homemade liquid cell was used.[46] The measurements were carried out by employing a Hewlett-Packard impedance/material analyzer 4291A integrated with a Tabai Espec temperature chamber SU-240-Y in the temperature range 235−400 K.

3. Results and Discussion

3.1. Overall Behavior. Figure 1 shows the frequency dependence of the real (a) and imaginary (b) part of the dielectric permittivity for homopolymer B_{63} ($M_n = 4500$ g mol^{-1}) at four temperatures (shown in the plots). As seen in the figure, two relaxation processes contribute to the dielectric dispersion, as the $\epsilon''(f)$ curves consist clearly of two peaks. The high-frequency peak is related to the dynamic glass transition of the oligomer (main relaxation), whereas the low-frequency peak is assigned to the normal mode process, further evidence for that assignment being provided by the results which follow. As the temperature is increased, the underlying motional processes become faster and their magnitude decreases, more pronouncedly for the normal mode process. The wide frequency range in our dielectric susceptibility measurements allow us to investigate both relaxations across a wide range of temperature.

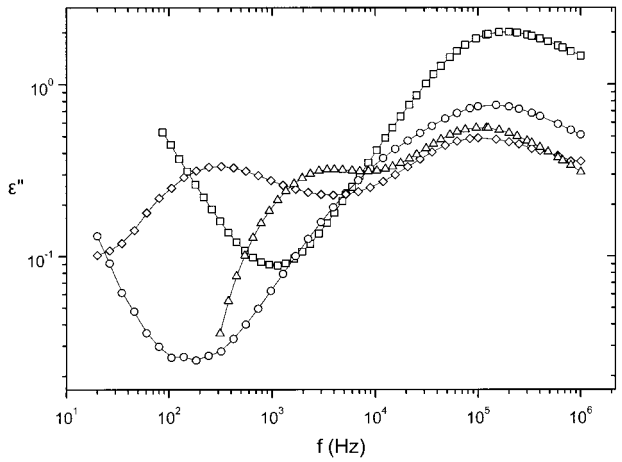

Figure 2. Imaginary part, ϵ'', of the dielectric permittivity, ϵ^*, vs frequency f at $T = 243$ K for homopolymers B_6 (M_n = 460 g mol^{-1}) (□), B_{14} (M_n = 970 g mol^{-1}) (○), B_{25} (M_n = 1810 g mol^{-1}) (△), and B_{63} (M_n = 4500 g mol^{-1}) (◇).

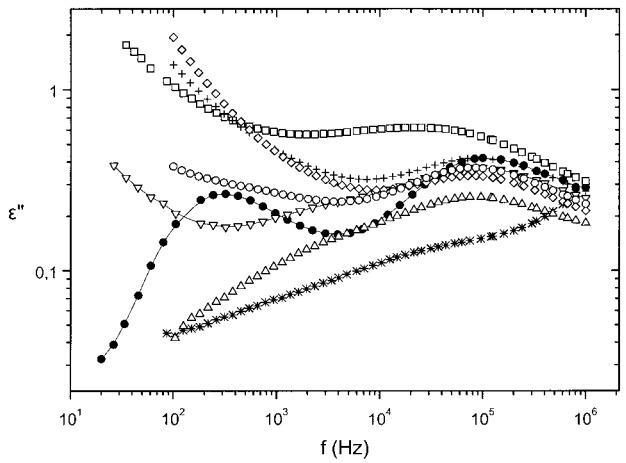

Figure 3. Imaginary part, ϵ'', of the dielectric permittivity, ϵ^*, vs frequency f at $T = 243$ K for copolymers $E_{32}B_3$ (*), $E_{30}B_7$ (□), $E_{32}B_{10}$ (△), $E_{26}B_{13}$ (▽), $E_{27}B_{17}$ (◇), $E_{29}B_{20}$ (+), and $E_{31}B_{30}$ (○). Results for B_{63} (●) are included for comparison.

Dielectric measurements were performed on four homopolymers (B_6, B_{14}, B_{25}, and B_{63}, see Table 1). $\epsilon''(f)$ plots for the homopolymers, at 243 K, are given in Figure 2. The peak at high frequencies in Figure 2 is assigned to the main relaxation, and it appears in the spectra of all four oligomers. The low-frequency peak, clearly observed only for B_{25} and B_{63}, is assigned to the normal mode process which reflects the motion of the whole chain. For B_6 the corresponding peak does not appear, whereas for B_{14} analysis of the spectrum using fitting procedures reveals the existence of the normal mode process.

The positions of the loss maxima arising from segmental motions (high-frequency peak, main relaxation) are almost independent of M_n, while the magnitude of the process (ϵ''_{max}) decreases drastically with increase in M_n. The normal mode process shows a pronounced dependence on molar mass, and there is a critical value, M_c, which serves as a lower limit for the appearance of this mode. For $M < M_c$ this process either is not activated or cannot be resolved from the α-relaxation. Our results show that for homopoly(B) M_c lies between 500 and 1000 g mol^{-1}. For comparison, M_c was found to be about 1000 g mol^{-1} for PPO.[9,25] In addition (as concluded from Figure 2 and discussed in detail later) the maxima of the $\epsilon''(f)$ plots shift to lower frequencies, and the magnitude of the process increases with increase in M_n.

In Figure 3 we show the frequency dependence of the imaginary part of the dielectric permittivity for the EB copolymers, compared with the $\epsilon''(f)$ plot of homopolymer B_{63}, all at a fixed temperature 243 K. The plots exhibit different contributions with increase in B-block length in the copolymer (i.e., with increase in n). We note here that we assume that E-blocks do not contribute to the relaxations exhibited by the copolymers. The degree of crystallinity of E-blocks is higher than 0.70,[30] and no significant contribution to the main relaxation is expected from the small noncrystalline fraction.[47] However, the E-units, which emerge from the lamellar surfaces of E-blocks and are connected to B-chains, could affect the motion of the whole B-chain. We describe briefly the main features of the spectra.

For sample $E_{32}B_3$ there is only one weak relaxation in the $\epsilon''(f)$ spectrum at 10^4-10^5 Hz, i.e., at frequencies lower than the peak frequency, f_{max}, of the peak related to the main relaxation in homopoly(B).

For $E_{30}B_7$ ($M_{n,B-block} \approx 500$ g mol^{-1}) the conductivity was remarkably high. Only one peak is observed in the $\epsilon''(f)$ plot. Analysis using the fitting procedure revealed that two relaxation processes contribute to the whole $\epsilon''(f)$ plot. We emphasize here that due to overlapping of the peaks, fitting procedures were necessary for the decomposition of the measured $\epsilon^*(f)$ data into the two relaxations and, usually, a conductivity contribution. We comment on the details of this analysis in discussing the following Figure 4.

For $E_{32}B_{10}$ ($M_{n,B-block} \approx 720$ g mol^{-1}) the $\epsilon''(f)$ plot in Figure 3 clearly consists of two contributions, the main peak showing a shoulder on the low-frequency side. Sample $E_{26}B_{13}$ ($M_{n,B-block} \approx 940$ g mol^{-1}) shows similar behavior to that of $E_{32}B_{10}$: two relaxations contribute clearly to the overall dielectric dispersion at 243 K and, in general, at low temperatures. At high temperatures conductivity effects masked the detailed features of the $\epsilon''(f)$ plots, especially at low frequencies.

For samples $E_{27}B_{17}$ and $E_{29}B_{20}$ conductivity effects dominate at low frequencies, even at $T = 243$ K, and only one relaxation peak is resolved. The position of this loss maximum coincides for both copolymers, and with the maximum of the high-frequency loss peak for the homopolymer B_{63}, which is assigned to the main relaxation. However, decomposition of the $\epsilon''(f)$ curves using the fitting procedure revealed the existence of the normal mode process for these copolymers.

For $E_{31}B_{30}$ we observe that two relaxation peaks are resolved. Decomposition of the $\epsilon''(f)$ plots into the two relaxations shows that the low-frequency peak has the same frequency of maximum as the normal mode process of homopolymer B_{63}. Similarly, also f_{max} for the high-frequency peak (main relaxation) coincides with that for B_{63}.

We note that the conductivity effects vary in magnitude among the samples. High ionic conductivity may originate from catalyst residues (residual potassium salts), the amounts of which will vary from sample to sample. Conductivity effects are strongly influenced by the long-range morphology of the sample (length scales from a few chain units to the dimensions of the specimen, depending on the frequency of observation). Reduction of crystallinity leads, as a general rule, to higher ionic conductivity, particularly so when considering ionic conduction in PEO-based systems where conduction is

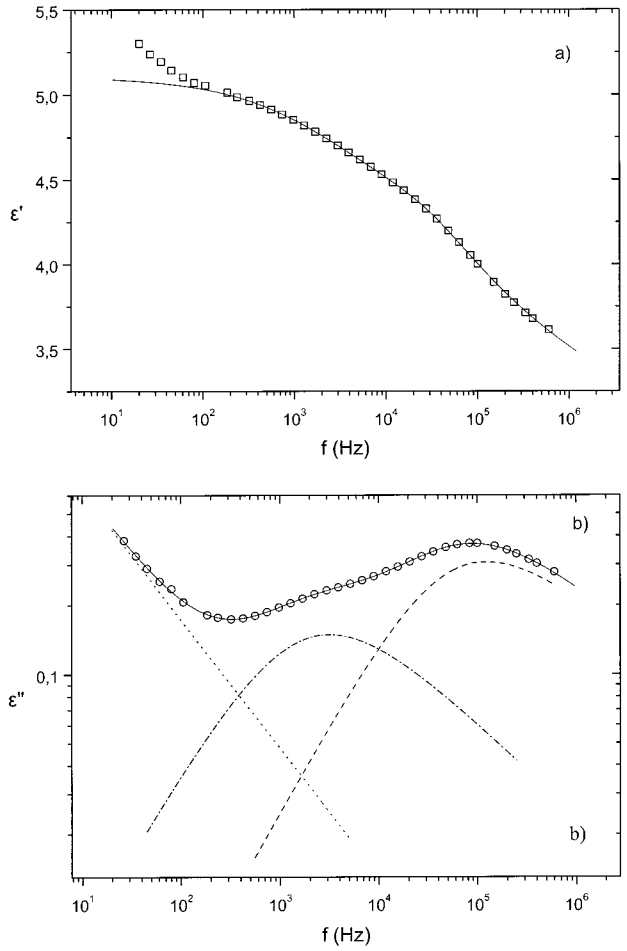

Figure 4. Real part, ϵ' (a), and imaginary part, ϵ'' (b), of the dielectric permittivity, ϵ^*, vs frequency f for copolymer $E_{26}B_{13}$ at $T = 243$ K. The solid lines are best fits of the HN equation (eq 9) to the data. In (b) we show the decomposition of the data into the main relaxation (dashed line), into the normal mode relaxation (dashed−dotted line), and into the conductivity contribution (dotted line).

generally acknowledged to take place though the noncrystalline PEO phase.[48] A smaller contribution would be expected from conductivity through the noncrystalline B phase. Structural studies of the present solid copolymers by SAXS, WAXS, and mainly by DSC have shown that there is a trend of decreasing crystallinity in the E-blocks with increase of B-block length up to $n = 17$: i.e., for $E_{27}B_{17}$ the fractional crystallinty shows a minimum, with a value of $x \approx 0.62$, and increases again to $x \approx 0.75$ for $n = 30$.[28,30] In Figure 3, it is seen that copolymer $E_{27}B_{17}$ exhibits the highest conductivity, consistent with the low crystallinity of its E-blocks. At this point we would like to note also that charge carrier motions are accompanied by polarization effects which give rise to an increase of the real part of dielectric permittivity, ϵ', at relative low frequencies (not shown here). The effects can be attributed to interfacial Maxwell−Wagner polarization mechanisms.[1] The structure of the investigated polymers is microphase separated where, moreover, one domain is semicrystalline. Thus, during the charge transport within the bulk of the materials, charge carriers can be trapped at the phase boundaries giving reason to interfacial polarization effects.

3.2. Fitting Procedure. In Figure 4 we present the experimental $\epsilon'(f)$ plot (Figure 4a) and $\epsilon''(f)$ plot (Figure 4b) for sample $E_{26}B_{13}$ at 243 K, together with the fit of the data incorporating the two-shape-parameters Havriliak−Negami function,[49] which yields an appropriate description of data in the vicinity of the peak frequency f_{max} of the dielectric loss $\epsilon''(f)$. For a quantitative analysis of the present dielectric spectra, a superposition of the two model functions according to Havriliak−Negami and of a conductivity contribution were fitted to $\epsilon^*(f)$:

$$\epsilon^*(f) = \sum_{k=1}^{2}\left[\epsilon_{\infty k} + \frac{\Delta\epsilon_k}{[1 + (if/f_{ok})^{1-\alpha_k}]^{\gamma_k}}\right] - i\frac{\sigma_{dc}}{\epsilon_0 f^s} \quad (9)$$

The second term on the right-hand side of eq 9 quantifies the dc conductivity σ_{dc}, which contributes only to imaginary part of $\epsilon^*(f)$ with the fit parameter (s) set to $s = 1$ for ohmic conductivity and $s < 1$ otherwise. ϵ_0 is the vacuum permittivity, ϵ_∞ is the limiting high-frequency permittivity, $\Delta\epsilon$ is the relaxation strength, and f_0 is the position on the frequency scale of the relaxation process. The index k ($k = 1, 2$) refers to the two processes that contribute to the dielectric response: normal mode and main relaxation in the order of increasing frequency. The exponents α and γ ($0 < (1 - \alpha)$, $(1 - \alpha)\gamma \leq 1$) define the symmetrical and asymmetrical broadening of the loss peaks, respectively, with respect to the Debye peak ($(1 - \alpha) = \gamma = 1$). Information on each relaxation process is obtained from the investigation of the temperature dependence of the relaxation rate of the process (Arrhenius plots), of the shape of the loss peak, and of its relaxation strength.

In several studies, simultaneous fitting of ϵ' and ϵ'' data has been shown to ensure maximum accuracy of the fitting procedure,[25,50] the results being better in the case where some characteristic parameters of the material under investigation are known (for example ϵ_∞). Looking at the Havriliak−Negami expression (eq 9), we find out that fitting of $\epsilon'(f)$ needs at least two more parameters, $\epsilon_{\infty n}$ (normal mode) and $\epsilon_{\infty\alpha}$ (main mode), in addition to the fitting parameters for the $\epsilon''(f)$ data. In the case where at low frequencies a power law frequency dependence of the real part of dielectric permittivity is also observed ($\epsilon'(f) \sim f^a$), two more parameters are necessary for the fit. In the general case, for low-frequency dispersion, the power law frequency dependencies of ϵ' and ϵ'' can be characterized by different fractional exponents.[51,52]

In Figure 4 the curves for the $\epsilon'(f)$ and $\epsilon''(f)$ plots were obtained by simultaneous fits of the real and imaginary part, keeping the ϵ_∞ parameters for the normal mode and the main relaxation as free parameters. The values of these parameters are very sensitive to the calibration and compensation procedures used for the different experimental setups. We note that for $\epsilon'(f)$ in Figure 4a we did not take into account the power law frequency dependence of ϵ' data at low frequencies during the fitting procedure, because that would have involved too many open parameters. In the case of $E_{26}B_{13}$ the procedure resulted in satisfactory fits, as shown in Figure 4. However, we point out that sometimes the simultaneous fit of wide range of ϵ' and ϵ'' data can result in unreasonable values of the many free parameters. Accordingly, the following strategy was adopted for the analysis of the experimental data throughout this work: first we fitted only the $\epsilon''(f)$ data over the whole frequency range, and afterward we attempted to fit the $\epsilon'(f)$ data, using the parameters obtained by the first fit, changing manually the strength parameters as

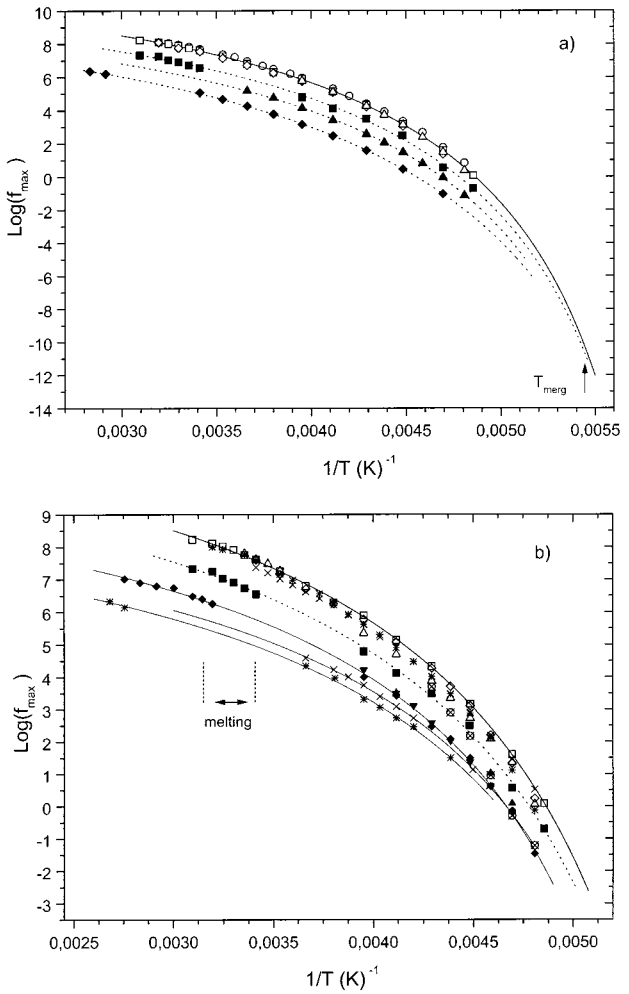

Figure 5. (a) Arrhenius plots (semilogarithmic plot of frequency of maximum dielectric loss, f_{max}, vs reciprocal temperature, $1/T$) for the main process (open symbols) and for the normal mode process (filled symbols) for homopolymers B_6 (○), B_{14} (□),B_{25} (△), and B_{63} (◇). Details in the text. (b) Arrhenius plots for the main process (open symbols) and for the normal mode process (filled symbols) for copolymers $E_{30}B_7$ (△), $E_{32}B_{10}$ (▽), $E_{26}B_{13}$ (◇), $E_{27}B_{17}$ (×), and $E_{31}B_{30}$ (*). Copolymer $E_{32}B_3$ (⊕) exhibits only one relaxation. Arrhenius plots for homopolymer B_{14} (□) are included for comparison. The lines are VFTH fits to the data. The temperature range of melting of E_mB_n copolymers is indicated in the plot.

required ($\Delta\epsilon_k$, $\epsilon_{\infty k}$ in eq 9). The new fit parameters were then used in a second fitting of the ϵ'' and ϵ' data. With this procedure we obtained reasonable and stable fit parameters.

3.3. Relaxation Frequencies: Effects of Temperature and Chain Length. All the $\epsilon^*(f)$ data were subjected to the fitting procedure according to eq 9, and the parameters that characterize the relaxation mechanisms were obtained. For all systems, the characteristic frequency f_{max} was derived from the Havriliak–Negami fit parameters (see eq 9) by the following equation[49]

$$f_{max} = f_0 \left[\frac{\sin\left[\frac{(1-\alpha)\pi}{2+2\gamma}\right]}{\sin\left[\frac{(1-\alpha)\gamma\pi}{2+2\gamma}\right]} \right]^{1/(1-\alpha)} \qquad (10)$$

In Figure 5 we give semilogarithmic plots of the peak frequency f_{max} versus reciprocal temperature $1/T$ (Arrhenius plots) for the main relaxation and the normal mode. In Figure 5a we show the Arrhenius plots for B homopolymers, while in Figure 5b the corresponding plots for the EB copolymers are given (the data for homopolymer B_{14} being included for comparison).

Table 2. VTFH Fit Parameters for the Main and Normal Mode Relaxations of B Homopolymers and EB Copolymers

	main relaxation			normal mode relaxation		
	log*A*	B	T_0/K	log *A*	B	T_0/K
Homopolymers						
B_6	11.79	1290	156.8			
B_{14}	11.62	1248	159.0	10.97	1407	153.2
B_{25}	10.78	1003	166.1	9.98	1276	158.0
B_{63}	11.55	1248	159.7	9.60	1485	152.4
Copolymers						
$E_{30}B_7$	12.71	1670	150.1	10.51	1243	161.2
$E_{32}B_{10}$	10.65	921	170.7	10.11	1249	161.0
$E_{26}B_{13}$	11.23	1116	164.0	9.50	1094	164.1
$E_{27}B_{17}$	12.0	1495	151.4	8.87	1111	159.4
$E_{29}B_{20}$	11.22	1204	160.0	10.5[a]	2175	125
$E_{31}B_{30}$	11.77	1300	160.2	8.68	1190	155.4

[a] Limited number of experimental points and mostly at high temperatures compared to T_g.

3.3.1. Homopolymers: Effect of Temperature. For the B homopolymers the temperature dependencies of both characteristic relaxation frequencies were well described (see Figure 5a) by the Vogel–Fulcher–Tammann–Hesse (VFTH) equation,[53–55]

$$f_{max} = A \exp\left(-\frac{B}{T - T_0}\right) \qquad (11)$$

where the preexponential factor (A), the activation parameter (B), and the Vogel temperature (T_0) are temperature-independent empirical parameters. The obtained VFTH fit parameters are given in Table 2. Consideration of Figure 5a and the fitting parameters in Table 2 leads to the conclusion that the dynamics of the segmental relaxation is almost independent of M_n while that of the normal mode process depends strongly on M_n. More specifically, the peak frequency of the latter decreases significantly with increase in M. Regarding the main relaxation, more detailed examination of the VFTH parameters in Table 2, as well as of the plots in Figure 5a, leads to the conclusion that there is a weak dependence of the main relaxation dynamics on M_n: the parameter T_0 (related strongly to T_g)[55] decreases slightly with increasing M_n, and so does also f_{max}.

Using Arrhenius plots, similar to those in Figure 5, it is possible to determine the so-called "dielectric glass transition temperature", $T_{g,diel}$, by the condition $\tau_\alpha(T_{g,diel}) = 100$ s.[4,56] For several systems $T_{g,diel}$ has been found to be similar to the calorimetric T_g and to follow its trends.[57] The values of $T_{g,diel}$ estimated for the four homopolymers are listed in Table 3. The error due to the fitting procedure is estimated to less than ±2 K. The results suggest a slight increase of the glass transition temperature with increasing M_n, as is expected for polymers that are not in the entanglement regime,[9] although the differences are within the estimated experimental error.

Several studies have appeared in the literature concerning the relationship between the segmental relaxation and the normal mode relaxation on the basis of dielectric measurements.[11,38,39] The temperature dependence of the characteristic time scales τ_α and τ_n of

Table 3. Characteristic Temperatures for B Homopolymers and EB Copolymers

	$T_{g,diel}$/K	T_{merg}/K
	Homopolymers	
B_6	195.2	
B_{14}	196.5	191
B_{25}	197.0	189
B_{63}	197.5	183
	Copolymers	
$E_{30}B_7$	197	
$E_{32}B_{10}$	200.4	196
$E_{26}B_{13}$	198.5	
$E_{27}B_{17}$	195.3	
$E_{29}B_{20}$	196.7	
$E_{31}B_{30}$	199.0	195.5

the main relaxation and of the normal mode process, respectively, and the merging of the two time scales at temperatures close to T_g have been the subject of these studies. Schönhals and co-workers have shown that the normal mode and the main relaxation merge at low temperatures for poly(propylene oxide) and polyisoprene.[9,11] Recent results by Adachi et al. confirm these findings, and the authors give an extensive discussion on the relationship between these two relaxations.[39] In Figure 5a we show how merging of segmental and normal mode relaxation is realized for sample B_{14} (M_n = 970 g mol^{-1}): obviously the temperature dependence of the characteristic frequencies of the two relaxations is different, and the two time scales coincide at a temperature T_{merg} (shown in the plot). The estimated values of T_{merg} for the homopolymers are listed in Table 3. We observe that these values are higher than T_0 (Table 2) and lower than (but close to) $T_{g,diel}$ (Table 3).

At this point we would like to comment on the relationship between the dielectric main (α) relaxation and the underlying segmental chain motions. It is well established that for polymers that exhibit dipole moment parallel to the main chain the main relaxation has its origin in local motions of the perpendicular dipole moment, μ_B, of the monomer. So, through the main relaxation we dedect dielectrically the fluctuations of the μ_B dipoles of monomers that are moving in a cooperative way, i.e., the vectorial sum, μ'_B, of the μ_B dipoles in the cooperatively rearranging regions (cooperative unit). The motions of the chain segments can indirectly be probed by the study of these dipolar motions; however, the question of the exact relationship between the fluctuations of the μ'_B dipole of the cooperative unit and the motions of the corresponding chain monomers has to be raised, before any quantitative discussion of segmental chain mobility based on studies of the dielectrically active main relaxation. For our systems, there is no constant proportionality between the μ'_B vector and the corresponding subchain vector of the cooperative unit, independent of the size of the cooperative unit. Thus, configurations of segments can hardly be quantitatively related to the dielectric strength of the main relaxation, and to be more precice, the mobility of the dipole is not strictly related to the segmental chain mobility. However, for the time scale detected for the mobility of μ'_B dipole by the main relaxation $\tau_\alpha = 1/(2\pi f_{max_\alpha})$, we could assume that changes in the size of the ccoperative unit are reflected in changes of τ_α. Consequently, the relaxation time τ_α exhibits the same temperature dependence with the segmental motions of the chain and can provide in, addition, information about the size of the cooperative unit (or its changes) as the temperature is approaching T_g.

According to the concept of cooperatively rearranging regions introduced by Adams and Gibbs[58] for the main relaxation, we expect T_{merg} to decrease with increase in M due to the cooperativity of segmental motions.[11,54] The length scale of the main relaxation (the correlation length ξ) increases as the temperature is lowered and diverges at T_0 (eq 11). On the other hand, the length scale of the normal mode process is in the order of the dimensions of the whole macromolecule (end-to-end vector) and scarcely changes with temperature. At T_{merg} the two length scales become comparable; i.e., the size of the cooperative unit becomes comparable with the length scale of the whole macromolecule. Thus, at $T = T_{merg}$ holds

$$\xi(T_{merg}) \approx \sqrt{\langle R^2 \rangle} \tag{12}$$

and due to the fact that $\sqrt{\langle R^2 \rangle}$ increases with M, eq 12 leads to the conclusion that T_{merg} decreases with increase in M. Our data on B homopolymers show that T_{merg} decreases with increasing M_n (Table 3) and, thus, are consistent with this scenario.

3.3.2. EB Diblock Copolymers: Effect of Temperature. In Figure 5b Arrhenius plots are given for both the normal mode and the main process for the E_mB_n copolymers with different B-block lengths (different n values). Figure 5b is to be compared with Figure 3, in which the $\epsilon''(f)$ plots of the EB copolymers are shown.

Regarding the main relaxation, we observe that for B-blocks with $n \geq 7$ the dynamics of the relaxation with respect to characteristic time scale $\tau = 1/(2\pi f_{max})$ is independent of M_n and that the characteristic frequencies f_{max} are slightly lower than the corresponding frequencies found for the B homopolymers. We estimated characteristic temperatures $T_{g,diel}$ also for the copolymers, and the values are given in Table 3. Within experimental error the values of $T_{g,diel}$ of the copolymers are independent of B-block length, suggesting that the dynamics of the main relaxation in the copolymers does not depend on n. As we can observe in Table 3, the values $T_{g,diel}$ of the copolymers are around 198 K, i.e., slightly higher than those found for the homopolymers.

Copolymer $E_{32}B_3$ exhibits a different temperature dependence of the characteristic frequency f_{max}: with decreasing temperature the molecular mobility responsible for the loss peak in Figure 3 decreases from that of the segmental relaxation of all the other copolymers to that of the normal mode relaxation of copolymers with longer B-blocks ($n \approx 13$).

Regarding the normal mode process, as expected, the position of the loss maxima depends on the molar mass. Because of lack of ϵ'' data measured with the same experimental setup and calibration for the normal mode as well as for the main relaxation process at relatively high temperatures (usually $T > 253$ K), we did not always fit the experimental data to define the normal mode process at high temperature, to keep the accuracy of the fits as high as possible and the fit parameters intercomparable. The first important result from the Arrhenius plots in Figure 5b is that we observe the normal mode relaxation of the B-blocks in $E_{30}B_7$ (M_n of the B block around 500 g mol^{-1}), whereas it did not appear in the spectrum of the B_6 homopolymer (M_n = 460 g mol^{-1}); see Figure 2. This finding is a first

indication of a difference in the fluctuations of the end-to-end vector of a B_n chain in the free state (bulk liquid) and when confined in the lamellar microdomains between crystallized E-blocks in the solid copolymers. In this respect, it is interesting to note that measurements at high pressures (up to 2 GPa) revealed the appearance of the normal mode process in PPG with $M_n = 400$ g mol^{-1}, whereas at atmospheric pressure no trace of the normal mode process was observed for that molar mass.[24] Additionally, for $E_{32}B_{10}$ and $E_{26}B_{13}$ (B-block $M_n = 720$ and 940 g mol^{-1}, respectively), the normal mode relaxation clearly contributes to overall dielectric dispersion (Figure 3). The fitting of these data is satisfactory and accurate, giving an error in f_{max} of less than ± 0.3 decade.

By extrapolating the VFTH fits of f_{max} of the copolymers to low temperatures, we tried to determine the merging temperatures T_{merg} of their main and normal mode characteristic frequencies. The results are given in Table 3. For copolymers with short B-blocks, the VFTH fits of the main and the normal mode relaxations are parallel to each other and do not merge. $E_{32}B_{10}$ is an exception, but we note that the experimental data for this sample are limited to relatively high temperatures, as compared to T_g, and to a narrow frequency range. Only for $E_{31}B_{30}$ (the longest B-block studied) did the characteristic frequencies merge, and we determined $T_{merg} = 195.5$ K. We observe that this value of T_{merg} is higher than those found for the B homopolymers (see Table 3), although the $T_{g,diel}$ values are similar for copolymers and homopolymers.

The merging of $f_{max,\alpha}$ and $f_{max,n}$ (and of the corresponding relaxation times τ_α and τ_n, due to the relation $\tau = 1/(2\pi f_{max})$) is related to the temperature dependence of the corresponding chain motions. Regarding the main relaxation, the experimental fact that for the homopolymer B_6 ($M_n \sim 500$ gr/mol) the normal mode process cannot be resolved from the main process, i.e., the time scales of the two processes coincide, implies that the length scales are also comparable. By the assumption that the τ_α time scale is related also to the size of the cooperative unit, we conclude that 4−6 monomer units could constitute the cooperative rearranging region (the whole chain consisting of six monomer units). Similar order of size for the cooperative unit is also suggested by the study of the B-blocks in the copolymers: the main relaxation for $E_{23}B_3$ copolymer is strongly retarded by decrease of temperature, approaching the time scale of the normal mode processes exhibited by longer B-blocks (Figure 5b), while for the $E_{30}B_7$ copolymer the main relaxation is remarkably slower compared to that for longer B-blocks and for the homopolymers. These results indicate that for short B-blocks, consisting of less than about seven monomers, the main relaxation is different from that for longer POB chains, implying that the cooperative units are of the size of 3−7 monomers (comparable to the whole chain length for the short B-blocks).

The merging of τ_α and τ_n indicates different temperature dependence of the mobility of the two underlying molecular processes, i.e., with decreasing T τ_α slows down more rapidly than τ_n does (due to the $\zeta(T)$ dependence, where ζ is the friction coefficient), probably due to an increase also of the size of the cooperative unit approaching T_g. Interchain cooperativities can also exist, so that the increase of the cooperatively rearranging regions related to the main process does not affect the

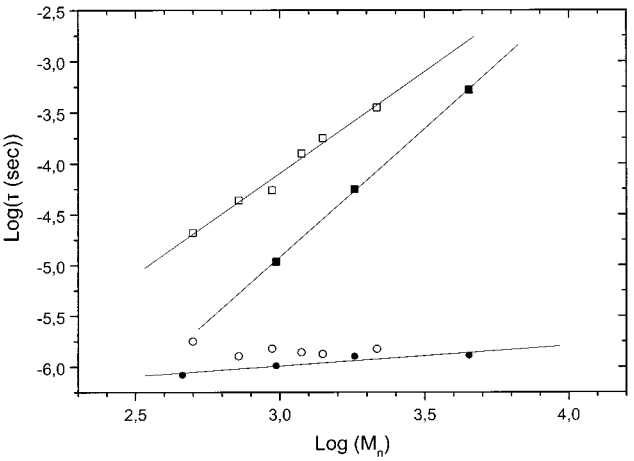

Figure 6. Dependence of nominal dielectric relaxation time, τ, at 243 K on molar mass, M_n, for the normal mode process (copolymers (□) and homopolymers (■)) and for the main process (copolymers (○) and homopolymers (●)). The lines are best linear fits to the data.

temperature dependence of the whole chain motions (normal mode process). In the case where no merging is observed, the temperature dependences of τ_α and τ_n are similar, approaching T_g. This can be attributed either to a limited increase of the cooperative unit (or at least due to the fact that the dipole moment μ'_B is not retarded drastically by the decrease of temperature) or to an influence of the increased cooperative unit to the whole chain motions and, consequently, to the temperature dependence of τ_n.[39] At this stage the explanation is not straightforward; however, the assumption that only intrachain cooperativities exist could be the key for the understanding of the strong correlation between the "freezing"of segmental motions and the mobility of the whole chain.

3.3.3. Nominal Relaxation Times: Effect of Chain Length. Considering Figure 5b, it is observed that the normal mode process for the confined B-blocks in the copolymers is retarded compared to the normal mode relaxation of the corresponding B homopolymers; i.e., f_{max} is larger for a homopolymer than for a copolymer with a B-block of comparable length (refer to Table 1 for corresponding molar masses of the B-blocks). To discuss this observation in a quantitative way, we determine average relaxation times, τ_α and τ_n for the segmental and the normal mode processes, respectively, using the relation $\tau = 1/(2\pi f_{max})$, where f_{max} is the characteristic relaxation rate of a relaxation.

In Figure 6 we show $\log(\tau_\alpha)$ and $\log(\tau_n)$ at 243 K versus $\log(M_n)$ for the B homopolymers and for the B-blocks of the diblock copolymers. Focusing our attention on the normal mode process, we observe a linear dependence of $\log(\tau_n)$ on $\log(M_n)$ for the EB copolymers. The best linear fit reveals the relation

$$\log \tau_n = -10.2 + 2.0 \log M_n \qquad (13)$$

i.e., the τ_n scales with molar mass according to $\tau_n \sim M^s$ with $s = 2 \pm 0.1$. For the homopolymers the exponent is slightly higher, $s = 2.50 \pm 0.05$, and the equation that describes the data is

$$\log \tau_n = -12.5 + 2.50 \log M_n \qquad (14)$$

Regarding the relaxation time τ_α (at 243 K) given in Figure 6, we observe, as we have already mentioned

with respect to Figure 5b, that they are independent of B-block length and that they are slightly higher in the copolymers compared with the homopolymers. For τ_α of the homopolymers we have drawn the linear fit to the data to emphasize the slight increase of τ_α with M_n at fixed temperature (i.e., increase of T_g with M_n). The data are well described by the equation

$$\log \tau_\alpha = -6.6 + 0.20 \log M_n \qquad (15)$$

We estimated the relaxation times for the normal mode process at three different temperatures, 223, 243, and 293 K, for the B homopolymers and for the B-blocks of the copolymers. The exponents s for the copolymers at the three temperatures are

$$T = 223 \text{ K}, s = 1.95 \pm 0.1; T = 243 \text{ K}, s = 2.03 \pm 0.05; T = 293 \text{ K}, s = 2.10 \pm 0.1$$

whereas the corresponding exponents for the homopolymers are

$$T = 223 \text{ K}, s = 2.60 \pm 0.05; T = 243 \text{ K}, s = 2.50 \pm 0.05; T = 293 \text{ K}, s = 2.35 \pm 0.1$$

We observe that for the copolymers the relation $\tau_n \sim M_n^{2.0 \pm 0.1}$ holds over a large temperature range, including the relatively low temperature of 223 K, which is close to T_g ($T_g \approx 210$ K). Thus, the choice of $T = 243$ K as a representative temperature (Figures 2, 3, and 6) is fully justified. For the homopolymers the exponent s decreases slightly with increasing temperature.

As shown in Figure 6, τ_n of the copolymers are longer than those of the homopolymers. For all temperatures and molar masses studied we get the relation

$$\tau_{n,cp}/\tau_{n,hp} \approx 4 \qquad (16)$$

where subscript "cp" denotes diblock copolymer and subscript "hp" denotes homopolymer. In other words, the molecular mobility for the whole PBO chain is retarded in the copolymers. However, for a detailed discussion of this observation, it is necessary to discuss the distributions of relaxation times of τ_n in the diblock copolymers and in the homopolymers. It is known that for the normal mode process the relaxation time τ_1 of the first mode (the slowest time) characterizes the time scale of the process in susceptibility measurements (see the Introduction). The value of τ_n estimated from the f_{max} values is an average relaxation time. It is established that it is close to τ_1, but the question of the exact relationship between τ_n and τ_1 has been addressed.[18] The controlling factor for that relationship is the distribution of the dielectric eigenmodes which contribute to the dielectric losses. As it is seen in eq 3, this distribution is characterized by the span of relaxation times τ_p and the g_p distribution. The distribution of relaxation times obtained by studying the frequency dependence of $\epsilon''(f)$, as described by the parameters ($1 - \alpha$ and γ) of the Havriliak−Negami equation, could serve as a guide for the distribution of the relaxation modes. Furthermore, to discuss the observed molar mass dependence of the nominal relaxation time τ_n in terms of theoretical models and their respective predictions, we should previously study the relationship between τ_n and τ_1. This is necessary because theoretical models, like the Rouse or the reptation model, predict the molar mass dependence of the longest relaxation mode (τ_1).

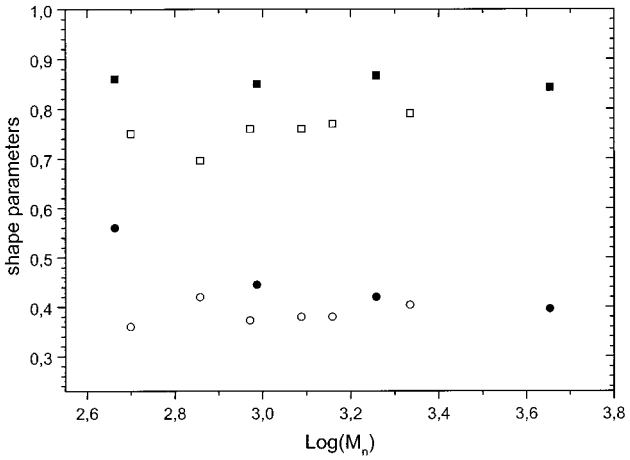

Figure 7. Molar mass dependence of the shape parameters, m_α and n_α, for the main process at 243 K, for E_mB_n copolymers (m_α (□), n_α (○)) and B_n homopolymers (m_α (■), n_α (●)).

3.3.4. Shape Parameters of the $\epsilon''(f)$ Curves. The fractional parameters $1 - \alpha$ and γ in the HN expression (eq 9) are related to the slopes of ϵ'' at low and high frequencies with respect to f_{max}:[43]

$$m = 1 - \alpha = \frac{\partial(\log \epsilon'')}{\partial(\log f)} \quad \text{for } f \ll f_{max} \qquad (17)$$

$$n = (1 - \alpha)\gamma = \frac{\partial(\log \epsilon'')}{\partial(\log f)} \quad \text{for } f \gg f_{max} \qquad (18)$$

In Figure 7 we plot the shape parameters, m_α and n_α, for the main relaxation at 243 K against $\log(M_n)$ for the homopolymers and the B-blocks of the copolymer. For the main relaxation the shape parameters were found to be independent of temperature. The scatter of data for the copolymers in Figure 7 serves as an indication of the uncertainty in the estimation of shape parameters using the fitting procedure. The high conductivity term in $\epsilon''(f)$ plots introduces a high degree of uncertainty in the estimation of the shape parameters of the main as well as of the normal mode process during the fitting procedure, this being more pronounced for the copolymers.

The shape parameter m_α is about 0.85 for the homopolymers, while the corresponding m_α values for the copolymers are scattered around a mean value of $m_\alpha \sim 0.77$. This parameter is a measure of the symmetrical broadening of the distribution of relaxation times: $m_\alpha = 1$ for a Debye relaxation mechanism. The slight decrease in the value of m_α of the copolymers compared to that for the homopolymers suggests a small influence of the confinement of B-blocks of the copolymer on their segmental motion. Yao et al.[18] have investigated the dielectric behavior of styrene−isoprene diblock copolymers in comparison with free homopolyisoprene. We follow a similar methodology and compare our results with theirs, despite significant differences between the two systems. We comment on these differences at a later stage (section 3.3.5). Regarding the main relaxation, they concluded that the copolymers and homopolymers were characterized by the same distribution of relaxation times. This result is in agreement with our finding that only a small broadening of the distribution of relaxation times occurs for the B-blocks in the copolymers compared to the B homopolymers.

The shape parameter n_α (Figure 7) is constant with respect to M_n, for the copolymers, with a mean value

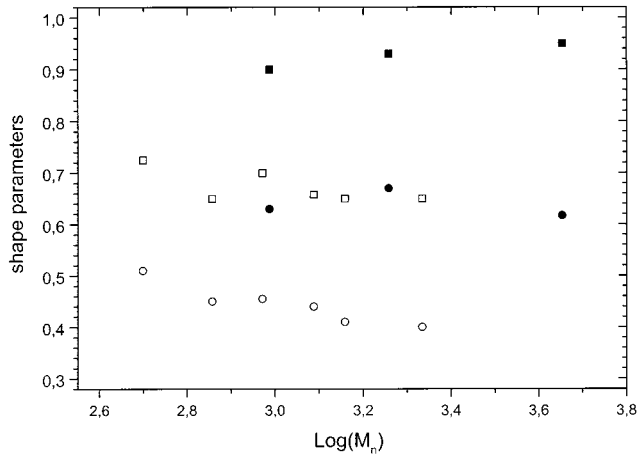

Figure 8. Molecular weight, MW, dependence of shape parameters, m_n and n_n, for the normal mode process, at 243 K, for copolymers (m_n (□), n_n (○)) and oligomers (m_n (■), n_n (●)). The dashed line is the best linear fit to the data; details are in the text.

$n_\alpha \approx 0.38$ and a similar degree of scattering as for the m_α parameter. For the homopolymers, the results suggest a decrease of n_α with increase in M_n, from 0.56 to 0.41. By definition, $n_\alpha = m_\alpha \gamma$, and consequently, (since m_α is constant, $m_\alpha \approx 0.85$) the parameter γ for the main relaxation of the homopolymers decreases from 0.65 to 0.48 (approximately) with increase in M_n. For the copolymers the corresponding values of the γ parameter are around 0.5. The γ parameter in the HN expression is a measure of the asymmetry of the distribution of relaxation times, having a value $\gamma = 1$ for the Debye and Cole−Cole relaxations (symmetrical functions). Therefore, our data show that the main relaxations of free B_n chains and B_n chains in solid copolymers exhibit similarly asymmetrical distributions of relaxation times, at least for the major part of the B−Block lengths studied, but a slightly broader distribution in the case of the copolymers.

In Figure 8 we present the shape parameters m_n and n_n, which characterize the normal mode process in the homopolymers and copolymers at 243 K. Regarding the m_n parameter for the homopolymers, we observe that the values are close to unity, as expected by the theory (see Introduction) and as has been found experimentally for the normal mode process in other systems.[10,11] This value suggests a very narrow distribution of relaxation times, in other words, that the first dielectric mode dominates the $\epsilon''(f)$ spectrum. The striking result in Figure 8 is that the m_n values found for the copolymers are significantly smaller, being scattered around a mean value of $m_n \approx 0.67$. This means that the normal mode process in the diblock copolymers has a broader distribution of relaxation times, resulting in a broadening of the $\epsilon''(f)$ curves compared to those of the homopolymers. The same effect was observed also by Yao et al. for diblock polyisoprene−polystyrene in comparison with homopolyisoprene.[18]

The values of the m parameter reflect the breadth of the loss spectrum and characterize also the frequency dependence of ϵ'' on the low-frequency side of the $\epsilon''(f)$ peak (eq 17). Usually, in dielectric relaxation spectroscopy the broadening of $\epsilon''(f)$ spectrum (decrease of m parameter) is interpreted as broadening of the distribution of relaxation times. In particular, for the normal mode relaxation it has been proposed that the broadening of the $\epsilon''(f)$ curves might be a direct consequence of enhanced intermolecular cooperativity.[59] More specifically, some authors tried to explain that broadening on the basis of the Ngai theory.[59,60] However, the comparison showed that the experimental findings are in disagreement with that theory.[59,60] Our data suggest also, in agreement with those studies, that this theory is not able to explain the broadening of the relaxation spectrum: possible enhancement of intermolecular cooperativity in the E_mB_n should affect also drastically the main relaxation (which is of highly cooperative character). However, the dynamics of the segmental relaxation of B-blocks has been found to be hardly affected in the copolymers. Therefore, another explanation should be sought for the broadening of the dielectric spectra in the copolymers. Recently, Watanabe et al.[12] explained these effects with changes in the distribution of dielectric modes which contribute to the relaxation spectrum. Such analysis could also explain our results, as will be explained in the following and in subsection 3.3.5.

For the B-blocks in the copolymers the frequency dependence of ϵ'' ($\epsilon'' \propto f^{0.67}$) is weaker than the linear dependence ($\epsilon'' \propto f^1$) for frequencies $f < f_{max}$ (in the frequency range studied). As is seen in eq 6 (Rouse model), ϵ'' exhibits a linear frequency dependence for time scales close to the longest relaxation time τ_1, this being characteristic for any model that predicts similar low-frequency terminal dynamics. Consequently, in the case of homopolymers the approximately linear frequency dependence of ϵ'' for $f < f_{max}$ implies that τ_n is close to the longest relaxation time τ_1, i.e., $\tau_{n,hp} \sim \tau_{1,hp}$. However, the weak frequency dependence of ϵ'' for the copolymers suggests that the nominal relaxation time $\tau_{n,cp}$ is not the longest time of the normal mode relaxation, i.e., $\tau_{n,cp} \ll \tau_{1,cp}$. This result may indicate that the chain dynamics of the B-blocks is strongly changed in the copolymers resulting in a significant change in the distribution of the dielectric eigenmodes in eq 3.

The n_n shape parameter corresponds to the power law frequency dependence of ϵ'' at high frequencies, $\epsilon'' \sim f^{-n}$ for the normal mode process. Our results for the homopolymers suggest that n_n is independent of M_n with a value close to 0.62. The exponent is higher than 0.5 (the value predicted by Rouse model, see Introduction). Regarding the copolymers, we observe that the values are dispersed around a mean value of $n_n \approx 0.45$ and are definitely lower than the values found for homopolymers ($n_n \approx 0.62$). Regarding the γ parameter and recalling that $n_n = m_n\gamma$, we estimate a value of $\gamma \approx 0.66$ for the homopolymers and $\gamma \approx 0.67$ for the copolymers (at 243 K). Therefore, we conclude that the asymmetry of the distribution of relaxation times for the normal mode process is similar in the two systems.

To summarize, we have found that the main relaxation of a B_n chain ($n \leq 30$) is scarcely affected by confining the B-blocks in the noncrystalline layers of stacked lamellae. The distribution of relaxation times is very narrow in the B homopolymers, becoming slightly broader in the solid copolymers. The asymmetry of the two distributions is similar. This being the case, comparison of the nominal relaxation times τ_α for the two systems is straightforward, as it reflects directly the relationship between the microscopic relaxation times. The small difference in τ_α in the copolymers compared to that in the homopolymers (Figure 6) can be attributed to changes in the environment of the polymeric chains in the two systems. We note also that the Arrhenius plots in Figure 5a,b do not reveal any

significant changes in $T_{g,diel}$, suggesting little effect of confinement on the dynamics of the main relaxation. With respect to the normal mode process the situation is significantly different. The dynamics of the global chain motion has been drastically affected by confining the B-blocks in microdomains between PEO crystallites.

3.3.5. Comparison of Normal Mode Dynamics in Homopolymers and Copolymers. Considering the copolymers and homopolymers, we have found that the normal mode dielectric loss curves in the copolymers are significantly broader compared to those in the homopolymers. Furthermore, the nominal relaxation time τ_n has been found to be about 4 times longer for the copolymers as compared to the homopolymers. As was discussed in subsection 3.3.4, the broadening of the dielectric loss curve for the copolymers may imply that $\tau_{n,cp} \ll \tau_{1,cp}$. Thus, for the B-blocks it is not the first mode which is the most intensive mode. This finding indicates that drastic changes in chain dynamics occur in the confined B-blocks, resulting in significant changes in the dielectric mode distribution.

Recent experimental[12,22] and simulation[61] studies on bulk and solution of *cis*-polyisoprene (homo-PI) chains, with or without inversion of dipoles parallel along the chain contour, indicated that, for a specific range of homo-PI concentration, the eigenfunctions $f_p(n)$ are nonsinusoidal with respect to the submolecule coordinate n. Consequently, the Rouse model, as well as the other models that consider the sinusoidal form of $f_p(n)$, do not properly describe the detailed features of $f_p(n)$ and $g_p(n)$. Watanabe et al.[12,22] explained the broadening of dielectric relaxation spectrum for homo-PI upon increasing of PI concentration with those nonsinusoidal normal modes. More specifically, they showed that solely changes in $f_p(n)$ and not in τ_p span result in the broadening of the dielectric mode distribution inducing changes of the g_p intensities of the individual dielectric modes p. They speculated that, when strong thermodynamic interaction exists between the polymeric chains affecting the dynamics of the chains, Rouse-like eigenmodes of each chain are mixed into new nonsinusoidal eigenmodes.

In E_mB_n copolymers we expect that, on one hand, enhanced thermodynamic interaction exists between the B-blocks, to minimize density fluctuations, and, on the other hand, the B-blocks exhibit reduced conformational flexibility, due to the fact that the E-blocks crystallize, resulting in a fixed end for the POB subchains. Therefore, this thermodynamic and spatial confinement of B-blocks in the copolymers might lead to significantly nonsinusoidal f_p (n) and, consequently, to a dramatic change of the dielectric mode distribution in eq 3. Discussing several possible factors that could lead to broadening of the $\epsilon''(f)$ curves in diblock polystyrene−polyisoprene systems, Yao et al. concluded that thermodynamic rather than spatial confinement might be the reason for this effect.[18] Supporting this conclusion, their data show that the Rouse model cannot satisfactorily describe the dynamics of polyisoprene blocks, in agreement with our findings. However, it is not straightforward to compare polystyrene−polyisoprene copolymers with E_mB_n copolymers at low temperatures. Because of the fact that the E-blocks crystallize, conformational flexibility is much less in E_mB_n copolymers than in a microphase-separated liquid state. Thus, more significant changes in eigenfunctions $f_p(n)$ could be expected for the E_mB_n system.

In our semicrystalline EB copolymers, the B-blocks are restricted in microdomains between lamellar of crystalline E-blocks (especially so at low values of n). A liquid-crystal model has been used to describe their conformation, i.e., the B-blocks in an array similar to a layer in a smectic liquid crystal which is formed because the orientation of chains emerging from the lamellar-crystal end surface is maintained through the B-block layer.[30,32] It seems that this orientation of the B-blocks (spatial confinement) affects strongly the whole-chain motion. It seems that each chain probes a different environment in the semiordered microphase between the crystalline lamellae. On the other hand, the study of segmental motions (main relaxation) shows that in this microphase there are no drastic changes in the short range interactions of segments compared to free homopolymer chains. We conclude that mainly the large-scale motions are affected. Another factor that could cause different behaviors of B-blocks and free chains could be a higher density of PBO in the lamellar microphase of the solid copolymers, which would probably mean an increase of interaction between chains and so a decrease of m_n for the copolymers, as observed (Figure 8). But then it should also, and mainly, affect the main relaxation and T_g, and this is not observed. The distribution of B-block and E-block lengths is another possible factor which could affect the normal modes of the whole-chain motion. Given the block lengths and distribution widths involved (Table 1), the standard deviation of the E-block-length distribution will be 4 or 5 units, so the environments of the short B-blocks must differ. The flux of E-block ends emerging from the crystal surface will impose constraints on the motions of B-blocks in a random way. The structure has to be described by a three-phase model consisting of a crystalline, an amorphous, and a rigid amorphous phase (mesophase) between them. Consequently, a polydispersity of compositions of the subchains that contribute to the normal-mode relaxation and the existence of that mesophase could certainly have a strong influence on the normal mode process, whereas only a minor influence on the local-segmental motions would be expected.

Regarding now the molar mass dependence of the nominal relaxation time, τ_n, for the normal mode relaxation (Figure 6), only the data for the homopolymers ($\tau_{n,hp} \sim \tau_1$) could be safely discussed in terms of the Rouse or any other theoretical model. For the B-blocks, our previous analysis suggests that probably $\tau_{n,cp} \ll \tau_1$. Thus, the M_n dependence of $\tau_{n,cp}$ could be hardly compared with theoretical predictions. The data in Figure 6 for the $\tau_{n,hp}$ suggest that the exponent s in eq 8 is close to the value of 2.5. Within the framework of the Rouse model, which predict $s = 2$, this result implies increased interchain interactions for the homopolymers.[9,10] We mention here that the discussion of our results in terms of the Rouse model is justified, because the critical molar mass for entanglement is on the order of 10 000 g mol^{-1} for polyethers;[9] i.e., the samples studied here are not in the entanglement regime. On the other hand, it is known that for the Rouse model to be used, the chain should include many (more than 5, for example) Kuhn segments. For the homopolymers it has been estimated a value of 2.92 B units per Kuhn segment; i.e., the molar mass of the Kuhn segment is about 210 g mol^{-1}.[62] Using these values, the calculation shows that the Rouse model can be used for POB chains with $M_n > 1000$ g mol^{-1}, a

condition which holds for the homopolymers studied here.

3.4. Effect of Melting. The melting range of the copolymers (290−320 K) falls into the temperature range of our measurements. A typical case is copolymer $E_{26}B_{13}$ (see Figure 5), and it is of interest to discuss the behavior of its normal mode process in the solid and in the melt. In Figure 5b we show that the values of the characteristic relaxation frequencies, f_{max}, fit well to the VFTH equation (eq 11) over the whole temperature range. The experimental points are for the solid state ($T < 288$ K) and the melt state ($T > 323$ K). If a fixed end caused the retardation of relaxation times of the normal mode process in the copolymers, we should observe a discontinuity in the Arrhenius plot in the temperature range 291−311 K, the melting range of sample $E_{26}B_{13}$.[30] However, such a discontinuity is not observed.

Considering the normal mode relaxation, the E-blocks also exhibit a normal mode process in the melt state. An E-chain has a similar backbone to a B-chain and will exhibit similar normal modes in its motions. Consequently, in the melt state the appropriate molar mass for $E_{26}B_{13}$ is 2080 g mol^{-1} (see Table 1). The ratio of values of τ_n at 333 K for free polymers with molar mass 940 g mol^{-1} (B_{13}) and 2080 g mol^{-1} ($E_{26}B_{13}$) can be simply estimated, if it is accepted that τ_n scales approximately as M_n^2 (see Figure 6 and related discussion). Thus, we predict a ratio $\tau_{n,2080}/\tau_{n,940} \approx 4.9$, in reasonable correspondence with the retardation of τ_n caused by a fixed end in the solid state: $\tau_{n,cp}/\tau_{n,hp} \approx 4$. If we assume that also some noncrystalline E units, for example 2, take part to the motion of the B subchain in the copolymers, then the molar mass of the flexible chain becomes ≈1030 and the ratio $\tau_{n,2080}/\tau_{n,1030}$ is very nearly 4. Consequently, the Arrhenius logarithmic plot shows no large discontinuity on passing from the solid to the melt state; see Figure 5b. Copolymer $E_{26}B_{13}$ is a special case, because it happens that the retardation of relaxation times caused by melting (due to the increase of molar mass) is in the same order as that due to the constrains imposed (to B_{13} subchain) by the lamellar crystals. Investigation of the normal mode process in the melt state, as well as in the solid state, for copolymers with other ratio of m/n (length of E-blocks to length of B-blocks) is now in progress in order to confirm the influence of a fixed end on the global motion of the B-blocks in the diblock copolymers.

3.5. Dielectric Strength. The dielectric permittivity $\epsilon^*(f)$ in susceptibility measurements provides information also on the strength of dielectrically activated relaxations. Using fitting procedures for the decomposition of the experimental $\epsilon^*(f)$ data into the individual relaxations contributing to $\epsilon^*(f)$, we get the dielectric strength of each mechanism as the $\Delta\epsilon_k$ parameter in eq 9.

In Table 4 we present the values of the dielectric strength, $\Delta\epsilon_\alpha$, for the main relaxation for the B homopolymers and the B-blocks of the copolymers. For the copolymers we assume that only the B-blocks contribute to $\Delta\epsilon_\alpha$ due to the high degree of crystallinity of the E-blocks (higher than 0.70[30]). Accordingly, we normalized $\Delta\epsilon_\alpha'$ to the volume fraction of B-blocks in the sample, ϕ_B (Table 1), $\Delta\epsilon_\alpha' = \Delta\epsilon_\alpha/\phi_B$, making it comparable to the $\Delta\epsilon_\alpha$ values for B homopolymers. We note here that for a more rigorous study we should apply an effective medium correction[57] to the data for the copolymers in order to exactly relate the measured $\epsilon^*(f)$ values to the real $\epsilon^*(f)$ values for the B-blocks. In future work we will consider the effect of such a correction.

Table 4. Dielectric Strength, $\Delta\epsilon_\alpha$, for the Main Relaxation and $\Delta\epsilon_n$ for the Normal Mode Process and Root-Mean-Square End-to-End Distance, $\langle R^2\rangle^{1/2}$, for B Homopolymers and EB Copolymers

	M_n or $M_{n,B-block}$/ g mol^{-1}	$\Delta\epsilon_\alpha$ or $\Delta\epsilon_\alpha'$	$\Delta\epsilon_n$ or $\Delta\epsilon_n'$	$\langle R^2\rangle^{1/2}$/nm
		Homopolymers		
B_6	460	6.14		
B_{14}	970	2.57	0.35	0.55
B_{25}	1810	2.07	0.80	1.14
B_{63}	4500	1.97	0.91	1.91
		Copolymers		
$E_{30}B_7$	500	4.94	2.63	1.10
$E_{32}B_{10}$	720	3.75	1.16	0.87
$E_{26}B_{13}$	940	2.58	1.19	1.0
$E_{27}B_{17}$	1220	2.04	1.48	1.28
$E_{29}B_{20}$	1440	2.53	1.56	1.42
$E_{31}B_{30}$	2160	1.84	1.48	1.70

The values in Table 4 reveal a trend, both for the B homopolymers and for the B-blocks in the EB copolymers, of the dielectric strength decreasing with increase in M. Therefore, for such low molar mass polymers, the contribution of chain ends cannot be neglected. The dielectric strengths $\Delta\epsilon_\alpha'$ and $\Delta\epsilon_\alpha$ have similar values for the same M_n.

Equation 7 can be written

$$\Delta\epsilon = \frac{4\pi\mu_u^2\langle R^2\rangle}{(4\pi\epsilon_0)3kT}\frac{N_A\rho}{M} \qquad (19)$$

where $\langle R^2\rangle = \langle \mathbf{R}(0)\cdot\mathbf{R}(0)\rangle$ is the mean-square end-to-end length of B chain, μ_u is the dipolar moment per unit contour length of the chain, and the total dipolar moment is $\mu = \mathbf{R}\cdot\mu_u$ (vectors). Equation 19 enables dielectric strength measurements of the normal mode process to be used to obtain an estimation of $\langle R^2\rangle$, the main interest here being to compare with each other $\langle R^2\rangle$ in the homopolymers and the copolymers.

At this point we would like to comment on the applicability of eq 19 for the case of B-blocks in the copolymers. For our microphase separated copolymers, the POB subchains cannot fully relax at sufficiently long times and, in addition, the system exhibits anisotropy due to the fixed ends at the PEO lamellar surface. For that system a more detailed analysis[63] leads to the following relation for the $\Delta\epsilon_n'$

$$\Delta\epsilon_n' \propto \langle R_E^2(0)\rangle - \langle R_E(\infty)\cdot R_E(0)\rangle \qquad (20)$$

where R_E is a component of $\mathbf{R}$ in the direction of the electric field. Equation 20 implies that the experimental value of $\Delta\epsilon_n'$ is not directly related to the mean-square end-to-end length of the B-block, $\langle R^2\rangle$, but to a smaller component of this quantity. Therefore, when eq 19 is applied for the B-blocks in the copolymers, we can estimate only a low limit value for the $\langle R^2\rangle$ (underestimation) and not the actual value of the end-to-end length of the B-block. We will use eq 19 for the copolymers only in this sense.

In Figure 9 we plot the dielectric strength of the normal mode process, $\Delta\epsilon_n$, against log(M_n) for the B homopolymers and for the B_n-blocks in the EB copolymers. For the copolymers, $\Delta\epsilon_n'$ values were normalized by the volume fraction of B. We observe that the values

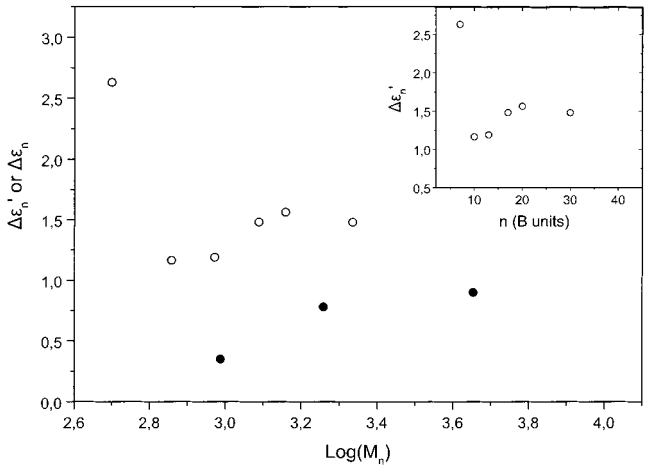

Figure 9. Molar mass dependence of dielectric strength, $\Delta\epsilon_n$, of the normal mode process for B homopolymers (●) and of normalized dielectric strength $\Delta\epsilon_n' = \Delta\epsilon_n/\phi_B$, of the normal mode process for E_mB_n copolymers (○). In the inset $\Delta\epsilon_n'$ is plotted against the B-block length (n in chain units) in the copolymers.

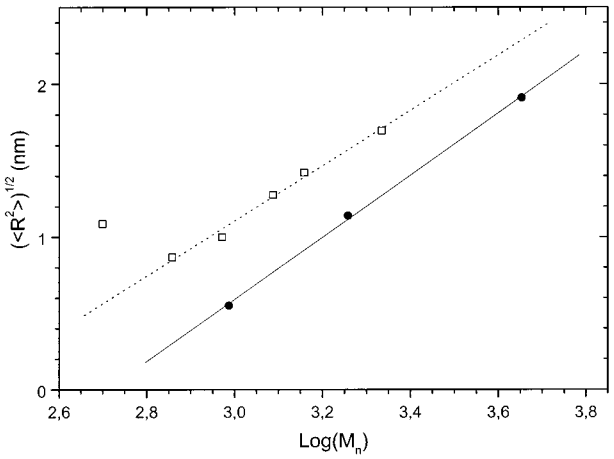

Figure 10. Dependence of end-to-end length $\sqrt{\langle R^2\rangle}$ of B_n chains in homopolymers (●) and of B_n blocks in E_mB_n copolymers (○). The lines are the best linear fits to the data; details are in the text.

of $\Delta\epsilon_n$ for the B homopolymers are clearly smaller than those of $\Delta\epsilon_n'$ for the copolymers. For the homopolymers, $\Delta\epsilon_n$ increases with M_n, as is expected from eq 7. For the B-blocks of the copolymers, the M dependence of $\Delta\epsilon_n'$ is rather complicated: for $n = 7$ the dielectric strength is relatively high, it decreases for $n = 10$, and then increases with M_n for $n > 10$. Finally, for $n = 30$ $\Delta\epsilon_n'$ decreases again: $\Delta\epsilon_n'$ is not as high as expected from the M dependence of $\Delta\epsilon_n'$ for lower n. This is seen more clearly in the inset in Figure 9, where we plot the dielectric strength versus the number of repeating units in the B-blocks. This plot clearly exhibits a discontinuity at $n = 30$ (copolymer $E_{31}B_{30}$).

The explanation of this behavior is not straightforward. From eqs 19 and 20 we conclude that $\Delta\epsilon_n'$ depends strongly on the mean-square end-to-end vector ($\langle R^2\rangle$) and also on the density ρ. Thus, two possible factors could lead to the discontinuity at $n = 30$: either a change in the density for that B-blocks length or a change in the molar-mass dependence of the mean-square of end-to-end vector or more accurately of the quantity $\langle R_E^2(0)\rangle - \langle R_E(\infty)\cdot R_E(0)\rangle$. However, the low dielectric strength for $n = 30$ cannot be explained solely by a change in ρ, since the density would need to increase by a factor of 2 or more to compensate for the higher M_n of the B_{30}. There is no indication of such a change in ρ for this copolymer.[30,32] Consequently, we attribute the change of $\Delta\epsilon_n'$ to a change in B-block conformation which occurs in the interval B_{20} to B_{30}. This is in agreement with the structural studies, which showed that the E-blocks in the lamellae of $E_{31}B_{30}$ are once folded, whereas those in $E_{29}B_{20}$ and shorter B-blocks were predominantly unfolded.[30,32] This E-block folding allows to the B-blocks to exhibit motions in a larger space, i.e., with less spatial constraints.

Supposing a largely trans-planar conformation for the B-blocks, the length per B unit along the chain is $l_B \approx 0.36$ nm.[30,32] We assume that the dipolar moment of a B unit is similar to that of an oxypropylene unit, i.e., $\mu = 1.4$ D (D) $= 1.4 \times 3.33 \times 10^{-30}$ Cb m,[64] and estimate $\mu_u = 1.3 \times 10^{-20}$ Cb for the dipolar moment per unit contour length of a B chain. Equation 19 leads to

$$\langle R^2\rangle = \frac{\Delta\epsilon_n 3kT 4\pi\epsilon_0 M}{4\pi N_A \rho {\mu_u}^2} \tag{21}$$

The density of liquid homopolymer B is 0.97 g cm^{-3} at 303 K, and there is still the question about the value of ρ in the copolymers.[32] However, density measurements on a related copolymer system[65] show that departures from normal density are not large, and we use $\rho \approx 1$ g cm^{-3} in eq 21 to obtain

$$\sqrt{\langle R^2\rangle} = \sqrt{0.09\Delta\epsilon_n M} \quad \text{in Å} \tag{22}$$

As discussed previously, eq 22 provides directly a value of the end-to-end length for the free B_n chain, whereas, it gives only suggestively a low limit value for the chain length of the B-blocks in the copolymers. In Table 4 we give the experimental $\Delta\epsilon_n$ (and $\Delta\epsilon_n'$) values and the estimated values of the square root of $\langle R^2\rangle$ we estimated (for homopolymers and copolymers). The root-mean-square end-to-end distance, $\langle R^2\rangle^{1/2}$, is plotted against log(M_n) for B homopolymers and for the B-blocks of the copolymers in Figure 10. It is seen that $\langle R^2\rangle^{1/2}$ for copolymer $E_{30}B_7$ is larger than expected and that, otherwise, $\langle R^2\rangle^{1/2}$ for the copolymers increases as M_n is increased. Values of $\langle R^2\rangle^{1/2}$ are smaller for the B homopolymers compared to those of the EB copolymers. Having in mind that for the copolymers the estimated $\langle R^2\rangle^{1/2}$ length is only a rough approximate low-limit value of the end-to-end length of the B-blocks, we conclude that the B-block conformation in the diblocks is highly expanded. The effect is more pronounced for short B-blocks. This is in agreement with the crystal/liquid-crystal model used to describe the solid-state structures of EB copolymers with short B-blocks, as discussed earlier (section 3.3.5).

Finally we comment on the values of $\langle R^2\rangle^{1/2}$ given in Table 4 in relation to the correlation length $\xi(T_{merg})$, as defined in terms of $\langle R^2\rangle^{1/2}$ in eq 12 of section 3.3.1. Our data suggest a value for ξ of 1−2 nm at a temperature slightly lower than $T_{g,diel}$. This value is in the order of values predicted for the correlation length at the glass transition.[54]

4. Summary and Concluding Remarks

Diblock copolymers of ethylene oxide and 1,2-butylene oxide, denoted $E_{30}B_n$, with constant E-block length of

30 units and various B-block lengths (B_n, $n = 3-30$) were investigated in parallel to B homopolymers with molar mass $M_n < 4500$ g mol^{-1}. Using dielectric relaxation spectroscopy, information was extracted for both the main and normal mode relaxations of the low-molar-mass homopolymers and copolymers in bulk. Information on molecular mobility and on conformations of polymer chains was derived mainly from two average quantities of the $\epsilon^*(f)$ spectra: the frequency of maximum dielectric loss in isothermal dielectric susceptibility measurements (f_{max}, sensitive to mobility) and the dielectric strength of the relaxation (sensitive to chain conformation). The information on chain conformation supplements previous structural studies.

With respect to the main relaxation, and comparing the dynamics of free chains in the liquid homopolymers with confined B-blocks in the lamellar stacks of the solid copolymers, our results show that the segmental motions are similar in the two systems. The distribution of relaxation times has similar asymmetry in both systems, but that of the copolymers is slightly broader. Regarding the magnitude of the peak in the $\epsilon^*(f)$ spectra associated with the main relaxation, similar values of the dielectric strength $\Delta\epsilon_\alpha$ were obtained for both systems, as well as the same dependence of $\Delta\epsilon_\alpha$ on M_n.

With respect to the normal mode relaxation, our results suggest that large-scale motions are drastically affected by confining the B_n chains in the lamellar stacks lamellae of the crystalline copolymers. Regarding the molecular mobility, the important experimental findings are summarized below:

(1) The critical molar mass for the appearance (or the separation from the main process) of the normal mode process, M_c, is lower for B-blocks in the copolymers ($M_c < 500$ g mol^{-1}) compared with B hompolymer ($M_c > 500$ g mol^{-1}).

(2) The dynamics of the free chains in the liquid homopolymers is described more appropriately by the Rouse model. However, the nominal dielectric relaxation time τ_n scales as $M_n^{2.5}$, implying enhanced interchain interactions. The dynamics of the B-blocks in the crystallized copolymers is drastically modified, resulting in significantly nonsinusoidal eigenfunctions $f_p(n)$ and different distribution of relaxation modes.

(3) The distribution of relaxation times was found to be broader for the B-blocks in the crystallized copolymers compared to that in the homopolymers. However, in both systems the degree of the asymmetry of the distribution of relaxation times is the same, the fractional exponent in the Havriliak−Negami equation being $\gamma \sim 0.66-0.67$.

(4) The global chain mobility of the copolymers is retarded as compared to that of the homopolymers, and the relation $\tau_{n,cp}/\tau_{n,hp} \approx 4$ holds across the whole molar mass range studied. On the other hand, the present results suggest that for the slowest relaxation times $\tau_{1,cp} \gg \tau_{1,hp}$.

(5) For the liquid oligomers, merging of the nominal relaxation times of the main, τ_α, and normal mode, τ_n, relaxations was observed at temperatures T_{merg} which were slightly lower than the dielectric glass transition temperature, $T_{g,diel}$. A similar effect was observed for copolymer $E_{31}B_{30}$ (the longest B-block studied) but not for the other copolymers ($B_n \leq 20$).

Regarding the dielectric strength of the normal mode relaxation, the changes in chain conformation are reflected in the following experimental finding.

(6) The normalized dielectric strength, $\Delta\epsilon_n'$, in the crystallized copolymers was higher than the corresponding dielectric strength in the liquid homopolymers, resulting in estimation of higher end-to-end lengths for the B_n chains in the copolymers.

The results from the dielectric strength of the relaxations indicate that the B_n blocks in the solid copolymers are expanded and oriented. The results are in agreement with the crystal/liquid-crystal model proposed previously to describe the structure of solid E_mB_n copolymers with short B-blocks.[30,32] According to this model, the B-blocks form an array similar to that in a smectic liquid crystal due to the orientation of the chains emerging from the lamellar-crystal end surface. Thus, the parallel orientation of E-blocks in the crystal is extended to the B-block microphase.

The broadening of the dielectric spectra and the increased normalized dielectric strength of the normal mode relaxation process in the crystallized copolymers imply that the B-blocks exhibit drastically different chain dynamics (configurations and mobility) compared to that of free polymeric chains. In agreement with recent experimental studies,[12] the dielectric behavior of confined B-blocks might be explained with significantly nonsinusoidal eigenfunctions $f_p(n)$ contributing to dielectric modes.

Dielectric measurements on copolymer $E_{31}B_{30}$ show that the molecular mobility and configuration of the B_{30}-blocks are different from those of shorter B-blocks ($n \leq 20$). In particular, the B_{30}-block is less expanded than the shorter blocks, and the relaxation times τ_α and τ_n do merge at low temperatures, contrary to what happens for the other copolymers, indicating a different relationship between segmental and global polymeric motions. These results support the conclusion from structural studies that in copolymer $E_{31}B_{30}$ E-block folding results in an increase in the volume available to the B-block. Dielectric measurements on E_mB_n copolymers with higher m and n values (now in progress) should provide additional information, mainly on the conformations of the B-blocks, but indirectly on the E-block lamellar structure.

The correlation length ξ, i.e., the characteristic length for the main (segmental) relaxation process, was estimated to be approximately 1−2 nm on the basis of observation of merging of the characteristic times of the main and normal processes at low temperature, i.e., at temperatures slightly (25−30 K) higher than the critical temperature T_0 in the VFTH equation. The finding that no merging of the characteristic relaxation times was observed for short B-blocks spatially restricted in the solid copolymers at low temperatures remains to be explained.

Acknowledgment. We thank Dr. V. M. Nace for his gift of the homopolymers used in this work. Thanks also to Dr. Siriporn Tanodekaew and Dr. Yung-Wei Yang, who prepared some of the copolymers, and to Ms Chiraphon Chaibundit, who prepared one of the homopolymers. The Engineering and Physical Science Research Council (UK) provides financial support for work on block copolymers at Manchester. A.K. and P.P. thank Dr. N. Bonanos, Risø National Laboratory, Roskilde, Denmark, for the liquid cell for high-frequency measurements and for helpful discussions concerning the relevant measurements. Finally, we thank the referees for critical and stimulating comments.

References and Notes

(1) McCrum, N. G.; Read, B. E.; Williams, G. *Anelastic and Dielectric Effects in Polymeric Solids*; Wiley: New York, 1967.
(2) *Dielectric Spectroscopy of Polymeric Materials*; Runt, J. P., Fitzgerald, J. J., Eds.; American Chemical Society; Washington, DC, 1997.
(3) Hofmann, A.; Kremer, F.; Fischer, E. W.; Schönhals, A. In *Disorder Effects on Relaxational Process*; Richert, R., Blumen, B., Eds.; Springer-Verlag: Berlin, 1994; p 309
(4) *Relaxation in Complex Systems*; Ngai, K. L., Riande, E., Ingram, M. D., Eds.*; J. Non-Cryst. Solids* **1998**, *235*−*237*.
(5) Bauer, M. E.; Stockmayer, W. H. *J. Chem. Phys.* **1965**, *43*, 4319.
(6) Stockmayer, W. H. *Pure Appl. Chem. Phys.* **1967**, *15*, 247.
(7) Imanishi, Y.; Adachi, K.; Kotaka, T. *J. Chem. Phys.* **1988**, *89*, 7593.
(8) Boese, D.; Kremmer, F. *Macromolecules* **1990**, *23*, 829.
(9) Schlosser, E.; Schönhals, A. *Prog. Colloid Polym. Sci.* **1993**, *91*, 158.
(10) Adachi, K.; Wada, T.; Kawamoto, T.; Kotaka, T. *Macromolecules* **1995**, *28*, 3588.
(11) Schönhals, A. *Macromolecules* **1993**, *26*, 1309.
(12) Watanabe, H.; Yamada, H.; Urakawa, O. *Macromolecules* **1995**, *28*, 6443. Watanabe, H.; Yao, M.-L.; Osaki, K. *Macromolecules* **1996**, *29*, 97. Urakawa, O.; Watanabe, H. *Macromolecules* **1997**, *30*, 652.
(13) Adachi, K.; Kotaka, T. *Prog. Polym. Sci.* **1993**, *18*, 585.
(14) Adachi, K.; Nishi, I.; Itoh, S.; Kotaka, T. *Macromolecules* **1990**, *23*, 2550.
(15) Fodor, J. S.; Huljak, J. R.; Hill, D. A. *J. Chem. Phys.* **1995**, *103*, 5725.
(16) Watanabe, H.; Yamazaki, M.; Yoshida, H.; Adachi, K.; Kotaka, T. *Macromolecules* **1991**, *24*, 5365.
(17) Alig, I.; Floudas, G.; Avgeropoulos, A.; Hadjichristidis, N. *Macromolecules* **1997**, *30*, 5004.
(18) Yao, M.-L.; Watanabe, H.; Adachi, K.; Kotaka, T. *Macromolecules* **1991**, *24*, 2955.
(19) Adachi, K.; Hirano, H.; Kotaka, T. *J. Non-Cryst. Solids* **1994**, *172*, 661.
(20) Kremer, F.; Boese, D.; Meier, G.; Fischer, E. W. *Prog. Colloid Polym. Sci.* **1989**, *80*, 129.
(21) Yoshida, H.; Watanabe, H.; Adachi, K.; Kotaka, T. *Macromolecules* **1991**, *24*, 2981.
(22) Watanabe, H.; Urakawa, O.; Kotaka, T. *Macromolecules* **1993**, *26*, 5073.
(23) Johari, G. P. *Polymer* **1986**, *27*, 866.
(24) Andersson, S. P.; Andersson, O. *Macromolecules* **1998**, *31*, 2999.
(25) Nicolai, T.; Floudas, G. *Macromolecules* **1998**, *31*, 2578.
(26) *Technical Literature, B Series Polyglycols. Butylene Oxide/ Ethylene Oxide Block Copolymers*; The Dow Chemical Co.: Freeport, TX, 1994.
(27) Nace, V. M. *J. Am. Oil Chem. Soc.* **1996**, *73*, 1.
(28) Hamley, I. W. *The Physics of Block Copolymers*; Oxford University Press: Oxford, 1998.
(29) *Nonionic Surfactants: Polyoxyalkylene Block Copolymers*; Nace V. M., Ed.; Marcel Dekker: New York, 1996.
(30) Yang, Y.-W.; Tanodekaew, S.; Mai, S.-M.; Booth, C.; Ryan, A. J.; Bras, W.; Viras, K. *Macromolecules* **1995**, *28*, 6029.
(31) Mai, S.-M.; Fairclough, J. P. A.; Hamley, I. W.; Matsen, M. W.; Denny, R. C.; Liao, B.-X.; Booth, C.; Ryan, A. J. *Macromolecules* **1996**, *29*, 6212.
(32) Mai, S.-M.; Fairclough, J. P. A.; Viras, K.; Gorry, P. A.; Hamley, I. W.; Ryan, A. J.; Booth, C. *Macromolecules* **1997**, *30*, 8392.
(33) Hamley, I. W.; Wallwork, M.-L.; Smith, D. A.; Fairclough, J. P. A.; Ryan, A. J.; Mai, S.-M.; Yang, Y.-W.; Booth, C. *Polymer* **1998**, *39*, 3321.
(34) Mai, S.-M.; Fairclough, J. P. A.; Terrill, N. J.; Turner, S. C.; Hamley, I. W.; Matsen, M. W.; Ryan, A. J.; Booth, C. *Macromolecules* **1998**, *31*, 8110.
(35) See, for example: Kelarakis, A.; Havredaki, V.; Derici, L.; Yu, G.-E.; Booth, C.; Hamley, I. W. *J. Chem. Soc., Faraday Trans.* **1998**, *94*, 3639 and references therein.
(36) Beevers, M. S.; Elliot, D. A.; Williams, G. *Polymer* **1979**, *20*, 785.
(37) Plazek, D. J. *Polym. J.* **1980**, *12*, 43.
(38) Ngai, K. L.; Schönhals, A.; Schlosser, E. *Macromolecules* **1992**, *25*, 4915.
(39) Adachi, K.; Hirano, H. *Macromolecules* **1998**, *31*, 3958.
(40) Rouse, P. E. *J. Chem. Phys.* **1953**, *21*, 1272.
(41) Doi, M.; Edwards, S. F. *The Theory of Polymer Dynamics*; Clarendon Press: Oxford, U.K., 1986.
(42) Scaife, B. K. P. *Principles of Dielectrics*: Clarendon Press: Oxford, U.K., 1989.
(43) Böttcher, C. J. F.; Bordewijk, P. *Theory of Electric Polarization*: Elsevier: Amsterdam, 1978.
(44) De Gennes, P.-G. *J. Chem. Phys.* **1971**, *55*, 572.
(45) Bedells, A. D.; Arafeh, R. M.; Yang, Z.; Attwood, D.; Heatley, F.; Padget, J. C.; Price, C.; Booth, C. *J. Chem. Soc., Faraday Trans.* **1993**, *89*, 1235. Tanodekaew, S.; Deng, N.-J.; Smith, S.; Yang, Y.-W.; Attwood, D.; Booth, C. *J. Phys. Chem.* **1993**, *97*, 11847.
(46) Bonanos, N.; Gunter, P. A.; Lumb, N. *Meas. Sci. Technol.*, to be published.
(47) Dobbertin, J.; Hensel, A.; Schick, C. *J. Therm. Anal.* **1996**, *47*, 1027.
(48) Armand, M. B. In *Polymer Electrolyte Reviews;* MacCallum, J. R., Vincent, C. A., Eds.; Elsevier: London, 1987; Vol. 1, Chapter 1.
(49) Havriliak, S.; Negami, S. *J. Polym. Sci., Polym. Symp.* **1966**, *14*, 89.
(50) Nowick, A. S.; Vayleyb, A. V.; Liu, W. *Solid State Ionics* **1998**, *105*, 121.
(51) Jonsher, A. K. *Universal Relaxation Law*; Chelsea Dielectric Press: London, 1996.
(52) *Impedance Spectroscopy*; Macdonald, J. R., Ed.; John Wiley: New York, 1987.
(53) Vogel, H. *Phys. Z.* **1921**, *22*, 645. Fulcher, G. S. *J. Am. Ceram. Soc.* **1925**, *8*, 339. Tammann, G.; Hesse, W. *Z. Chem.* **1926**, *156*, 245.
(54) Donth, E. *Relaxation and Thermodynamics in Polymers. Glass Transition*; Akademic Verlag: Berlin, 1992.
(55) DiMarzio, E. A.; Yang, A. J. M. *J. Res. Natl. Inst. Stand. Technol.* **1997**, *102*, 135.
(56) Ngai, K. L.; Roland C. M. *Macromolecules* **1993**, *26*, 6824.
(57) Daoukaki, D.; Barut, G.; Pelster, R.; Nimtz, G.; Kyritsis, A.; Pissis, P. *Phys. Rev. B* **1998**, *58*, 5336.
(58) Adam, G.; Gibbs, J. H. *J. Chem. Phys.* **1965**, *43*, 139.
(59) Schroeder, M. J.; Roland, C. M. *Macromolecules* **1999**, *32*, 2000.
(60) Adachi, K.; Hirano, H.; Freire, J. J. *Polymer* **1999**, *40*, 2271.
(61) Kaznessis, Y. N.; Hill, D. A.; Maginn, E. J. *Macromolecules* **1999**, *32*, 6679.
(62) Booth, C.; Orme, R. *Polymer* **1970**, *11*, 626.
(63) Cole, R. *J. Chem. Phys.* **1965**, *42*, 637. Williams, G. *Dielectric Spectroscopy of Polymeric Materials*; Runt, J. P., Fitzgerald, J. J., Eds.; American Chemical Society: Washington, DC, 1997; Chapter 1.
(64) Krigbaum, W. R.; Dawkins, J. V. Dipole Moments of Polymers in Solution. In *Polymer Handbook;* Brandrup, J., Immergut, E. H., Eds.; Wiley: New York, 1989; Vol. 7, p 493
(65) Ashman, P. C.; Booth, C. *Polymer* **1975**, *16*, 889. Ashman, P. C.; Booth, C.; Cooper, D. R.; Price, C. *Polymer* **1975**, *16*, 897.
(66) We thank one of the reviewers for bringing eq 20 to our attention.

MA990429E